Electric Power Systems Research 80 (2010) 1160–1170

Contents lists available at ScienceDirect

Electric Power Systems Research

journal homepage: www.elsevier.com/locate/epsr

A generalized model for the calculation of the impedances and admittances of overhead power lines above stratified earth

Theofilos A. Papadopoulos, Grigoris K. Papagiannis*, Dimitris P. Labridis

Power Systems Laboratory, Dept. of Electrical and Computer Engineering, Aristotle University of Thessaloniki, 54124 Thessaloniki, Greece

ARTICLE INFO

Article history:
Received 1 September 2008
Received in revised form 10 January 2010
Accepted 20 March 2010
Available online 24 April 2010

Keywords:
Earth return admittance
Earth return impedance
Multiconductor lines
Nonhomogeneous earth
Transient analysis

ABSTRACT

A general formulation for the determination of the influence of imperfect earth on overhead transmission line impedances and admittances is presented in this paper. The resulting model can be used in the simulation of electromagnetic transients in cases of two-layer earth over a wide frequency range, covering most fast transient phenomena of power engineering interest. The propagation characteristics of an overhead transmission line over homogeneous and two-layer earth are investigated using the proposed model. A systematic comparison of the proposed model with other approaches is also presented and the differences due to earth stratification are reported. Finally, the transmission line parameters calculated by the proposed formulation are used in the simulation of fast transient surges in a transmission line excited by double exponential sources.

1. Introduction

Overhead transmission line (TL) modelling in electromagnetic (EM) transient simulations requires the detailed representation of the influence of the imperfect earth on the conductor parameters. Although several approaches have been used since many years, the accurate modelling of earth conduction effects on transmission lines is still an appealing research topic, especially in the high frequency region for the simulation of fast transients.

Historically, the first approach is the Carson's homogeneous earth model [1]. Carson proposed the use of earth correction terms for the series impedances, which are derived using the following assumptions:

- The relative permeability of the homogeneous earth is considered to be equal to unity.
- The axial displacement currents in the air and in the earth are neglected.
- The influence of the imperfect homogeneous earth on the shunt admittances is neglected.
- Quasi-TEM (Transverse ElectroMagnetic) field propagation is assumed.

Carson's approach has been intensively used in the calculation of the series impedances of transmission lines. It provided a useful tool for TL modelling, especially in simulations where the displacement currents and the influence of the imperfect earth on shunt admittances can be neglected.

Many efforts to develop more accurate models, mainly for the earth return impedance calculation in high frequency region are reported in the literature, in these approaches the axial displacement currents are taken into account either using analytical formulas [2,3] or approximations. Among the latter are the asymptotic approach of Semlyen [4] and the logarithmic evaluation, originally proposed by Sunde [5] and extended in [6]. Discrepancies and limitations of these approximate models are discussed in [7,8].

A different approach, aiming at the calculation of the earth conduction effects on both the series impedances and the shunt admittances was proposed by Wise; the Herzian vector has been used to develop proper earth correction terms for both series impedances [9,10] and shunt admittances [11] for a single conductor. This semi-infinite homogeneous earth model was further improved by Nakagawa, who extended the formulas for the series impedances earth correction terms for cases of multiconductor lines and for earth configurations consisting of several horizontal layers with different EM properties, taking also into account the displacement currents in the earth [14]. The multi-layered earth model of Nakagawa is implemented in the Electromagnetic Transients Program (ATP-EMTP) [15]. Additionally Nakagawa proposed formulas for shunt admittances but only for the homogeneous earth case [12,13]. The shunt admittance formulation has been extended

* Corresponding author at: Power Systems Laboratory, Department of Electrical and Computer Engineering, Aristotle University of Thessaloniki, P.O. Box 486, 54124 Thessaloniki, Greece. Tel.: +30 2310996388; fax: +30 2310996302.
E-mail address: grigoris@eng.auth.gr (G.K. Papagiannis).

0378-7796/$ – see front matter © 2010 Elsevier B.V. All rights reserved.
doi:10.1016/j.epsr.2010.03.009

for the case of a two-layer earth by Ametani et al. [16] who also used a similar approach.

An attempt to find an exact solution to the problem was also suggested by Kikuchi [17]. In his work he investigated the transition from quasi-TEM to surface wave guide propagation. A similar approach has been adopted in [18,19]. Pettersson [20] used Kikuchi's formulas but instead of an asymptotic expansion he proposed logarithmic expressions, similar to Sunde for their numerical evaluation. This procedure has been adopted in [21,22], where a wide frequency TL model is proposed.

Wait extended Kikuchi's work in [23] by proposing an exact full wave model for a thin wire above homogeneous earth. Other attempts to extend this model to multiconductor arrangements are reported in [24,25].

Scope of this paper is to present a generalized model for the calculation of the influence of the imperfect earth on the impedances and the admittances of an overhead TL for the two-layer earth case. The analysis is based on the assumption of quasi-TEM field propagation. The EM field equations are solved using the Herzian Vector approach. The generalized expressions derived are evaluated numerically, using a proper numerical integration technique [26]. The formulation, presented in this paper, is a continuation in the development of impedance and admittance formulas, and includes most of the above mentioned approaches in a single, generalized model. A systematic and detailed comparison is implemented, marking the corresponding similarities and differences between the existing approaches and the proposed formulation. The proposed model can be used in a wide frequency range, covering most practical power engineering problems. Furthermore, the provided investigation points out the significance of displacement currents, admittance earth correction terms and earth stratification in the high frequency region.

The proposed formulation is applied to a typical single-circuit three-phase transmission line for the calculation of the propagation characteristics for different earth structures. The propagation modes are decomposed using modal transformations [27] and their modal characteristics are presented for frequencies from 50 Hz up to 10 MHz, covering a wide range of power engineering operational states, from steady state up to fast front transients, including applications of power-line communication. The obtained results are first checked against the relative results by other approximations for the case of homogeneous earth in order to justify the validity of the proposed methodology. Next, the influence of earth stratification is examined, by comparing the corresponding results to those for the semi-infinite earth cases. It is shown that the influence of earth permittivity on the earth correction terms for both the impedances and the admittances must be taken into account for frequencies higher than hundreds of kHz, especially for cases with a poor earth conductivity.

Finally, the transmission line parameters, calculated with the proposed methodology are used in typical EM transient simulations to investigate their impact on the transmission line transient responses.

The theoretical analysis, combined with the systematic numerical investigation offers a well defined and widely applicable model for the simulation of fast front transients in transmission lines.

2. Transmission line modelling

For a transmission line of N conductors in the frequency domain the following telegrapher's equations apply:

$$\frac{\partial \mathbf{V}}{\partial x} = -\mathbf{Z}'(\omega)\mathbf{I}, \tag{1a}$$

$$\frac{\partial \mathbf{I}}{\partial x} = -\mathbf{Y}'(\omega)\mathbf{V}. \tag{1b}$$

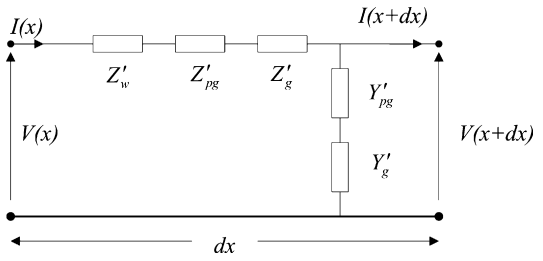

Fig. 1. Per-unit-length equivalent circuit of one conductor.

The N vectors $\mathbf{V}$ and $\mathbf{I}$ are the line voltages with respect to a reference conductor and line currents, respectively. Axis x is the longitudinal direction along the transmission line as shown in Fig. 1.

The $N \times N$ matrices $\mathbf{Z}'(\omega)$ and $\mathbf{Y}'(\omega)$ are the per-unit (pu) length frequency dependent series and shunt admittance matrices, respectively. These matrices consist of the following components [13]:

$$\mathbf{Z}'(\omega) = \mathbf{Z}'_{\mathbf{w}} + \mathbf{Z}'_{\mathbf{e}} = \mathbf{Z}'_{\mathbf{w}} + \mathbf{Z}'_{\mathbf{pg}} + \mathbf{Z}'_{\mathbf{g}}, \tag{2}$$

$$\boldsymbol{Y}'(\omega) = \boldsymbol{Y}'_{\boldsymbol{e}}(\omega) = j\omega \boldsymbol{P}_{\boldsymbol{e}}^{-1} = j\omega(\boldsymbol{P}_{\boldsymbol{pg}} + \boldsymbol{P}_{\boldsymbol{g}})^{-1}, \tag{3a}$$

$$\boldsymbol{Y}'_{\boldsymbol{pg}} = j\omega \boldsymbol{P}_{\boldsymbol{pg}}^{-1}, \tag{3b}$$

$$\boldsymbol{Y}'_{\boldsymbol{g}} = j\omega \boldsymbol{P}_{\boldsymbol{g}}^{-1}. \tag{3c}$$

$\mathbf{P}$ is the potential coefficient matrix. The other terms referred in the above equations are defined as:

- $\boldsymbol{Z}'_{\boldsymbol{pg}}$ and $\boldsymbol{Y}'_{\boldsymbol{pg}}$ are the pu length impedances and admittances, respectively, due to the influence of the perfectly conducting earth.
- $\boldsymbol{Z}'_{\boldsymbol{g}}$ and $\boldsymbol{Y}'_{\boldsymbol{g}}$ the pu length impedances and admittances, respectively, due to the influence of the imperfect earth.
- $\boldsymbol{Z}'_{\boldsymbol{w}}$ is the pu length diagonal internal impedance matrix of the conductor, calculated by the skin effect formulas [28].

The pu length equivalent circuit describing this system of equations is shown in Fig. 1 for the case of one conductor.

3. Self- and mutual impedances and admittances

3.1. Analytical formulation

For the calculation of the pu length parameters of an overhead conductor configuration, the general wire arrangement of Fig. 2 is considered, consisting of two uniform, electrically thin perfect conductors located in the air above the two-layered earth structure. The first layer has a depth d, while the lowest layer extends to infinity. The permittivity and permeability of air are ε_0 and μ_0, respectively. The permittivity of the first layer is ε_1, the permeability and conductivity are μ_1 and σ_1, respectively, while the corresponding characteristics of the second layer are ε_2, μ_2 and σ_2. Conductor i is of infinite length while conductor j is of pu length. The heights of the two conductors from the earth surface are h_i and h_j, respectively, and their horizontal distance is y_{ij}.

The pu length mutual impedance $Z_{e_{ij}}$ and admittance $Y_{e_{ij}}$ are derived in (4a) and (4b) using the Hertzian vector components Π'_{0x} and Π'_{0z} as explained in Appendix A. Integrating along the infinite conductor i, replacing h with h_i, z with $h_j + d$, y with y_{ij} and assuming the exponential law of propagation along the conductor with

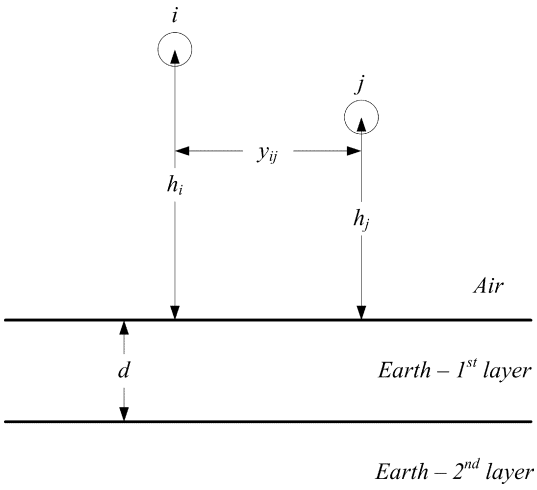

Fig. 2. Geometric configuration of two thin conductors above a two-layered earth.

propagation constant γ_x [5,9–11] results in:

$$Z'_{e_{ij}}(\gamma_x) = \frac{j\omega\mu_0}{4\pi} \cdot \int_0^\infty \left[\frac{u}{a_0}(e^{-a_0\left|h_j-h_i\right|} + e^{-a_0(h_j+h_i)} \cdot T'_1)\right] \times \left[\int_{-\infty}^{\infty} J_0(u\sqrt{x^2+y_{ij}^2})e^{-\gamma_x x}dx\right] du, \quad (4a)$$

$$Y'^{-1}_{e_{ij}}(\gamma_x) = \frac{j\omega\mu_0}{4\pi\gamma_o^2} \int_0^\infty \left[\frac{u}{a_0}(e^{-a_0\left|h_j-h_i\right|} + e^{-a_0(h_i+h_j)} \cdot T'_1) + 2a_0 u \cdot T'_2 \cdot e^{-a_0(h_i+h_j)}\right] \times \left[\int_{-\infty}^{\infty} J_0(u\sqrt{x^2+y_{ij}^2})e^{-\gamma_x x}dx\right] du, \quad (4b)$$

The integral expressions of (4a) and (4b) are very difficult to be evaluated numerically, due to the unknown propagation constant γ_x. In the literature [29] the existence of an additional discrete propagation mode is distinguished, characterized as *surface-attached* or *fast-wave* mode, besides the classical *transmission line mode*. However, a satisfactory approximation is the quasi-TEM propagation [21], where only the *transmission line mode* is assumed, and so γ_x can be taken equal to the propagation constant of the free space $\gamma_x = \gamma_0 = jk_0 = j\omega\sqrt{\varepsilon_0\mu_0}$ [20].

Assuming the quasi-TEM field propagation, the pul mutual impedance and admittance for the two-layer earth structure are derived be the procedure described in Appendix A and have the form of (5) and (6), respectively.

Pu length mutual impedance

$$Z'_{e_{ij}} = Z'_{pg_{ij}} + Z'_{g_{ij}} = \frac{j\omega\mu_0}{2\pi} \ln\frac{D_{ij}}{d_{ij}} + \frac{j\omega\mu_0}{\pi}(P + jQ), \quad (5a)$$

$$P + jQ = \int_0^\infty F_{strat}(\lambda) \cdot e^{-\lambda(h_i+h_j)} \cos(y_{ij}\lambda) \cdot d\lambda. \quad (5b)$$

$$F_{strat}(\lambda) = \mu_1 \frac{s_{12} + d_{12}e^{-2\alpha_1 d}}{s_{01}s_{12} + d_{01}d_{12}e^{-2\alpha_1 d}}, \quad (5c)$$

Pu length mutual admittance

$$Y'_{e_{ij}} = j\omega P^{-1}_{e_{ij}}, \quad (6a)$$

$$P_{e_{ij}} = P_{pg_{ij}} + P_{g_{ij}} = \frac{1}{2\pi\varepsilon_0} \ln\frac{D_{ij}}{d_{ij}} + \frac{1}{\pi\varepsilon_0}(M + jN), \quad (6b)$$

$$M + jN = \int_0^\infty [F_{strat}(\lambda) + G_{strat}(\lambda)]e^{-\lambda(h_i+h_j)} \cos(y_{ij}\lambda)d\lambda, \quad (6c)$$

$$G_{strat}(\lambda) = \lambda \frac{\mu_0\mu_1(\gamma_0^2-\gamma_1^2)(s_{12}+d_{12}e^{-2\alpha_1 d})(S_{12}+D_{12}e^{-2\alpha_1 d}) - 4\mu_0\mu_1^2\mu_2\alpha_1^2\gamma_0^2(\gamma_2^2-\gamma_1^2)e^{-2\alpha_1 d}}{\Delta_2 \cdot \Delta}, \quad (6d)$$

In the above equations λ is the new integral argument. The integral terms in (5) and (6) represent the influence of the imperfect earth on the conductor impedances and admittances. This is expressed by proper correction terms, following a notation similar to the original by Carson, which will be called *earth return correction terms* hereafter. Neglecting the conductor losses $\mathbf{Z_w}$ in (2), which can be calculated individually, the self-impedance and the self-admittance of conductor *i* of Fig. 2 are derived from (5) and (6), respectively, by replacing y_{ij} with conductor's outer radius and h_j with h_i.

The $G_{strat}(\lambda)$ function is due to radial displacement currents in the earth. Ignoring $G_{strat}(\lambda)$ results in a purely imaginary propagation constant and a lossless propagation above imperfect earth [22].

Eqs. (5) and (6) of the two-layer earth model are transformed to the corresponding generalized expressions for the homogeneous earth case, assuming that the electromagnetic properties of the two layers are the same and so $\gamma_2 = \gamma_1$, $a_2 = a_1$.

The proposed methodology can be extended further for the case of a multi-layered earth with arbitrary number of horizontal layers. In this case (5) and (6) become very complex, including terms which represent the relation of the electromagnetic characteristics between the layers.

Eqs. (5) and (6) include semi-infinite integrals. These can be evaluated numerically, using the integration scheme of [26], which is a combination of different methods. The proposed scheme has been proved to be very efficient numerically for the type of the integrands involved.

3.2. Frequency dependent behavior of earth

The proposed model includes the influence of axial displacement currents in all media and the influence of the imperfect earth on the pu length admittances for a generalized two-layer earth model. The significance of these parameters can be analyzed, considering the frequency dependent behavior of earth [17,18]. This frequency dependent behavior of earth may be classified for the homogeneous earth case, adopting Semlyen's criteria and the corresponding definition of the critical frequency f_{cr} [4].

$$f_{cr} = \frac{\sigma_1}{2\pi\varepsilon_0\varepsilon_{r1}} \text{ Hz}, \quad (7)$$

- If $f < 0.1f_{cr}$ the displacement currents are negligible and earth behaves as a conductor. This earth behavior is characterized as low frequency or Carson's region.
- If $0.1f_{cr} < f < 2f_{cr}$ the displacement and resistive currents are comparable and the earth behaves both as a conductor and as an insulator, or otherwise as a quasi-conductor. This earth behavior is characterized as high frequency or transition region.
- If $f > 2f_{cr}$ the displacement currents are predominant and the earth behaves as an insulator. This earth behavior is the very high frequency or Semlyen's region.

In Fig. 3 the plot of the minimum critical frequency $f_{cr,min} = 0.1f_{cr}$ for different values of the homogeneous earth relative permittivity ε_{r1}, shows the boundaries of the low frequency region. For frequencies above those boundaries, the influence of the displacement

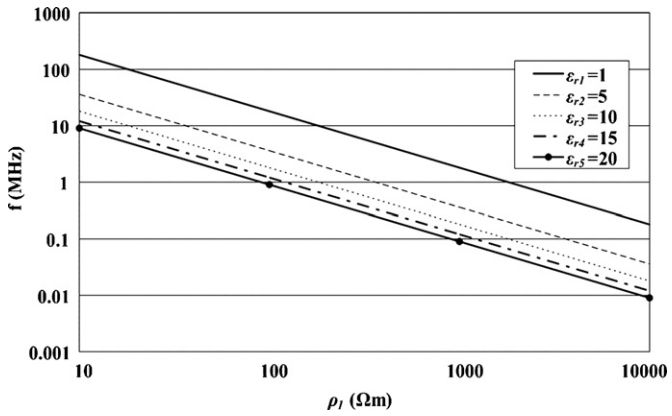

Fig. 3. Plot of $f_{cr,min}$ against earth resistivity for different relative permittivities of the homogeneous earth.

currents on both impedances [30] and admittances [17] should be taken into account and the expressions of (5) and (6) must be used.

The above boundaries may exceed the TL frequency limit, defined as $f \ll c/h$, where c is the speed of light and h is the height of the conductor above ground. However, for problems including the calculation of voltages and currents along the line or crosstalk phenomena, the TL approach can be a satisfactory approximation [21].

3.3. Comparison with other earth models

Eqs. (5) and (6) have a generalized form, capable of handling cases with arbitrary resistivities, permittivities, and permeabilities for each of the two earth layers. In this way other stratified and homogeneous earth models already proposed in the literature may be derived by applying the corresponding assumptions. Therefore:

3.3.1. Pu length impedances for the two-layer earth

- Omitting ε_0 in the air, setting $\mu_k = \mu_0$ and for arbitrary ε_k, relation (5) reduces to Sunde's formula for the two-layer earth model, disregarding the displacement currents in the air [5].
- For $\mu_k \neq \mu_0, \varepsilon_k \neq \varepsilon_0$, the generalized formulation of (5) is identical with that proposed in [14] for the case of the two-layer earth.

A systematic comparison of numerical results of the above earth impedance formulas is presented in [26].

3.3.2. Pu length admittances for the two-layer earth

Eq. (6) is similar to the two-layered earth model for the calculation of the earth return admittance, proposed by Ametani et al. [16].

3.3.3. Pu length impedances for the homogeneous earth

For $\mu_1 = \mu_0$ and $\varepsilon_1 = \varepsilon_0$, or otherwise neglecting μ_1, ε_1, μ_0 and ε_0, Carson's [1] formula is expressed, disregarding the displacement currents in the air and the earth.

Omitting ε_0 in the air, setting $\mu_k = \mu_0$ and for arbitrary ε_1, Sunde's formula is expressed for the homogeneous earth case, disregarding the displacement currents in the air [5,6].

For arbitrary μ_1, μ_0, ε_1, ε_0, the approaches of [2] and [3] are expressed.

3.3.4. Pu length impedances and admittances for the homogeneous earth

The formulas for the series impedances and admittances proposed independently by Wise in [9–11] and also investigated in [12,13] by Nakagawa, respectively, can be expressed by the proposed model.

The full wave model of Kikuchi [17] and Wait [23], developed for the homogeneous earth, is also expressed by the proposed model, assuming lossless propagation with velocity equal to the velocity of the free space. The electromagnetic scattering model, presented in [19] can also be expressed, under the assumption of field propagation in the conductor's plane.

Finally, the same expressions of the proposed homogeneous earth model have been applied by Pettersson [20]. However, Pettersson suggested an image type approach for the numerical evaluation of the impedance and admittance earth correction terms, using logarithmic approximations. His work has been also adopted in [21,22], where it is shown that it can be used sufficiently for frequencies up to 100 MHz, while several authors also use this model in Power-line Communication (PLC) applications for calculations of voltage profiles along the line or of crosstalk phenomena [31].

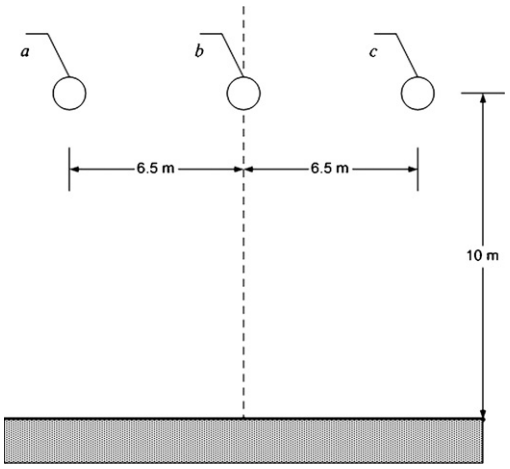

Fig. 4. 150 kV single-circuit three-phase overhead transmission line configuration.

4. System under test

4.1. Transmission line configuration

A typical horizontal single-circuit 150 kV overhead TL with ACSR conductors is used in the analysis. The geometrical configuration of the line is shown in Fig. 4, while the conductor data are presented in Table 1. The ground wires are treated like the conductor wires. However, since in the calculation of transient responses the equivalent phase conductors are used, the ground wires would have to be numerically eliminated. To avoid the possible introduction of errors, due to the numerical elimination and in order to have a better estimation of the influence of the earth on the actual phase conductors, the ground wires are neglected in this configuration.

4.2. Earth structures

In order to analyze all possible types of earth behavior, different two-layer earth models have been investigated, covering a wide

Table 1
Transmission line data.

Conductor type	ACSR
Inner diameter (mm)	10.714
Outer diameter (mm)	18.2
Conductor conductivity (S/m)	2.59×10^7
Relative permeability of conductor	1

Table 2
Earth conditions.

Case number	ε_{r1}	ε_{r2}
Homogeneous earth models		
H1	10	–
H2	20	–
Two-layer earth models		
S1	10	10
S2	20	20
S3	10	20
S4	20	10

range of topologies, where the ratio of the first to the second layer earth resistivity is $\rho_1/\rho_2 = 10, 5, 0.1, 0.2$, with $\rho_2 = 10, 100, 1000\ \Omega$ m. Different relative permittivities for the two layers are assumed from 1 to 20. The depth of the first layer is assumed to be variable, ranging between 5, 10 and 20 m, while the second layer is of infinite extent. The relative permeability of both layers is considered to be equal to unity, since most soil types are non-magnetic. The case of the homogeneous earth model is also examined for the same earth topologies as in the two-layer earth case, assuming that the electromagnetic properties of the two layers are equal. In Table 2 the most representative cases are presented for a ratio of ρ_1/ρ_2 equal to 10 and $\rho_2 = 100\ \Omega$ m for the two-layer earth and $\rho_1 = 1000\ \Omega$ m for the homogeneous earth.

5. Homogeneous earth analysis

The proposed expressions of the homogeneous earth are used for the calculation of impedance and admittance earth correction terms of the overhead line configuration of Fig. 4. The wave propagation characteristics are calculated by the application of proper modal decomposition [27].

First of all the validity of the results of the proposed model is checked by comparing them to the corresponding by [11,12,17]. For all cases examined and over the whole frequency range, all models gave identical results.

Then, the wave propagation characteristics are compared with the corresponding obtained by other approaches, which use different assumptions or numerical approximations. The first of them is Carson's model [1] since it is the most typical model used extensively for the calculation of the influence of the homogeneous earth return path on the TL impedances. The second model is Sunde's model [5], which is an extension of [1] and is proposed for the simulation of fast-wave transients in multiconductor configurations [8]. Finally the model proposed by Pettersson [20] is examined. Although this model adopts the same assumptions as in the proposed model, differences in the results occur, due to the different methods used for the numerical evaluation of the impedance and admittance earth correction terms, as explained previously. Furthermore a considerable drawback of the model of [20] is that it is limited only for cases of homogeneous earth.

The magnitude of the ground mode characteristic impedance and the attenuation constants of the ground and aerial #1 modes as a function of frequency are presented in Figs. 5–7, respectively, for the H1 case of Table 2.

The percent differences between the results for the attenuation constants are calculated using (8). The results by the proposed model are used as a reference. Similar differences are also calculated for the other propagation parameters as well as for the pul self-impedance and admittance of the conductor of phase *a* in Tables 3 and 4, respectively.

$$\text{Difference } (\%) = \frac{\left|\alpha_{\text{other model}} - \alpha_{\text{proposed}}\right|}{\left|\alpha_{\text{proposed}}\right|} \times 100, \tag{8}$$

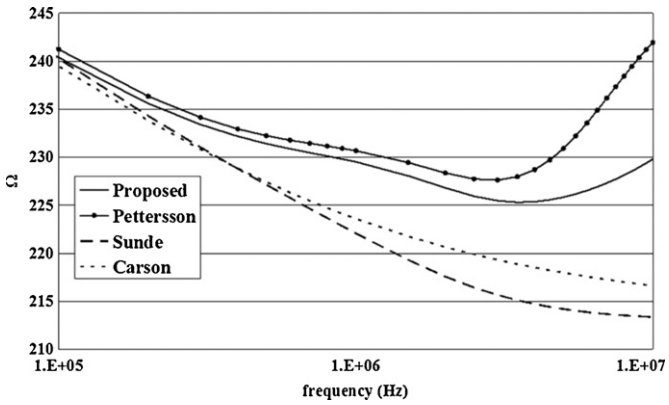

Fig. 5. Magnitude of ground mode characteristic impedance for the different approaches for the homogeneous earth.

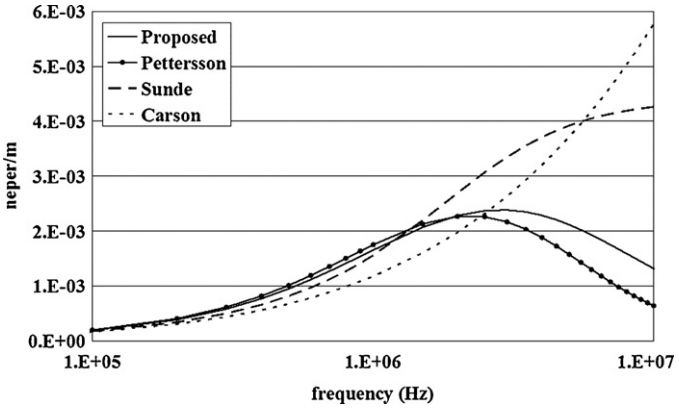

Fig. 6. Ground mode attenuation constant for the different approaches for the homogeneous earth.

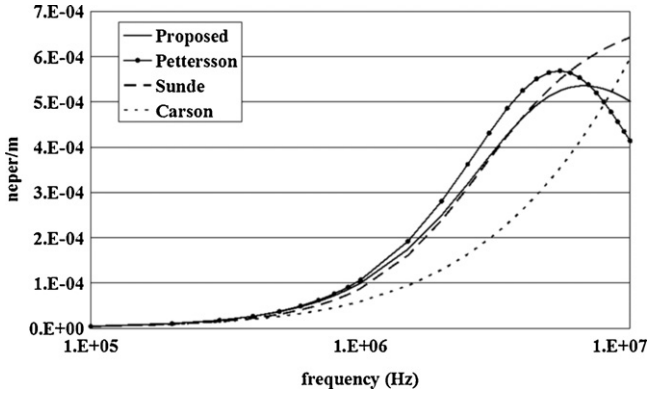

Fig. 7. Aerial mode #1 attenuation constant for the different approaches for the homogeneous earth.

Table 3
% Differences in the self-resistance and inductance of impedance Z_{11} using different approaches. Homogeneous earth case.

Frequency	Carson		Sunde		Pettersson	
	R_{11}	X_{11}	R_{11}	X_{11}	R_{11}	X_{11}
100 kHz	3.14	0.27	3.49	2.33	3.13	2.37
500 kHz	13.23	4.09	4.66	0.75	3.29	1.37
1 MHz	20.77	13.88	4.35	1.64	2.78	0.42
2.5 MHz	23.93	72.60	0.33	8.24	1.10	1.58
5 MHz	8.73	247.90	3.38	12.00	0.05	1.88
7.5 MHz	10.13	494.07	4.39	12.55	0.18	1.23
10 MHz	28.26	793.42	4.73	12.6	0.14	0.79

Table 4
% Differences in the self-conductance and susceptance of admittance Y_{11} using different approaches. Homogeneous earth case.

Frequency	Real part	Imaginary part
100 kHz	11.08	0.01
500 kHz	19.54	0.13
1 MHz	27.90	0.30
2.5 MHz	50.20	2.07
5 MHz	282.86	1.53
7.5 MHz	299.51	1.24
10 MHz	329.83	1.10

As shown in Figs. 6 and 7, the ground and aerial mode attenuation constants, calculated by the models of [1] and [5] are both monotonically increasing functions of frequency, while the corresponding results calculated with the proposed model are non-monotone functions.

Differences in the modal propagation constants between the models of Carson and the proposed are recorded for frequencies higher than the minimum critical frequency $f_{cr,min}$, which for the examined case is 180 kHz. For frequencies up to 1 MHz are attributed mainly to the differences in the pul impedances as shown in Table 3, due to the omission of the influence of earth permittivity [30], while for higher frequencies also due to the omission of the imperfect earth on the shunt admittances.

In Sunde's model the influence of earth permittivity is taken into account, thus differences in the modal attenuation constants, related to the small differences in the pul impedances of Table 3, have been reduced in the kHz range. The small differences in the pul parameters are due to the omission of the displacement currents in the air. However, the divergence of the results in the propagation terms in the MHz range is considerable, due to the omission of the influence of the imperfect earth on the shunt admittances.

The wave propagation characteristics obtained by [20] and by the proposed model are almost identical for frequencies up to 3 MHz, since differences do not overcome 10% for all wave parameters, since the differences in the pul impedances and susceptances are negligible. In the upper frequency range both models show the same behavior, while high differences are recorded mainly for the ground attenuation constant, since significant differences in the shunt conductances are recorded, as shown in Table 4.

In Table 5, the relative differences in the propagation characteristics are shown for different homogeneous earth cases of Table 2, assuming earth resistivity equal to 500 Ω m. Differences in the rest propagation characteristics are not significant [32] and so they are not presented.

Table 5
% Differences in the ground mode attenuation constant with different models. Homogeneous earth case.

Cases	Frequencies			
	500 kHz	1 MHz	5 MHz	10 MHz
Carson's model				
H1	22.17	27.31	35.53	221.57
H2	24.86	27.89	59.51	260.87
Sunde's model				
H1	13.15	14.14	60.95	199.71
H2	10.05	6.89	56.82	150.56
Pettersson's model				
H1	5.4	6.4	22.3	51.75
H2	5.01	4.83	17.17	43.08

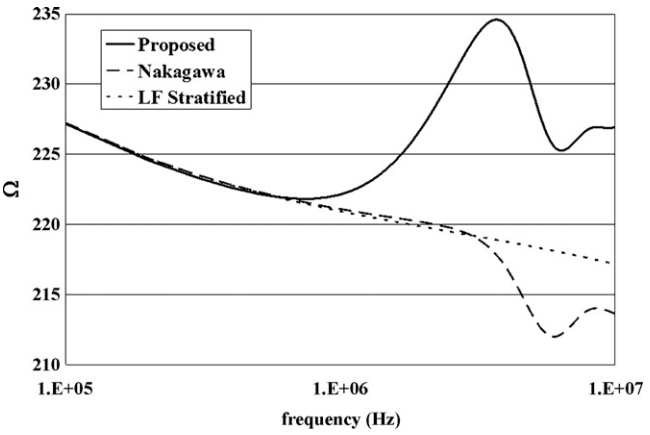

Fig. 8. Magnitude of ground mode characteristic impedance for different two-layer methods.

6. Two-layer earth analysis

As in the homogeneous earth case, the modal propagation characteristics of the proposed method are compared to those obtained by other approaches. The stratified earth topology for case S1, described previously, with depth of the first layer equal to 5 m is used in the following analysis.

First a simplified model is assumed, where both the influence of the permittivity of the earth and the influence of the admittance earth correction terms are neglected. This model, which is similar to Carson's model but suitable for stratified cases, will be characterized as "Low frequency (LF) Stratified earth model".

The second model is a slight improvement to the latter in the high frequency range, since it takes into account only the effect of the air and the earth permittivities on the earth impedances. This model is equivalent to that proposed by Nakagawa for the two-layer earth case.

The ground and aerial mode attenuation constants, calculated by the three models are presented in Figs. 9 and 10, respectively. The corresponding curves of the LF Stratified model are monotonically increasing functions with frequency, much similar to Carson's model for the homogeneous earth, since they both use the same assumptions. For the ground mode, significant differences are recorded for frequencies higher than the minimum critical frequency of the first layer. In the high frequency region the ground mode characteristics by the two models show a completely different behavior.

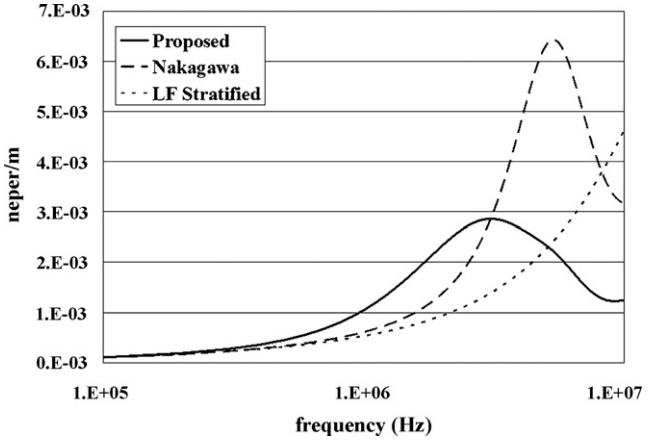

Fig. 9. Ground mode attenuation constant for different two-layer methods.

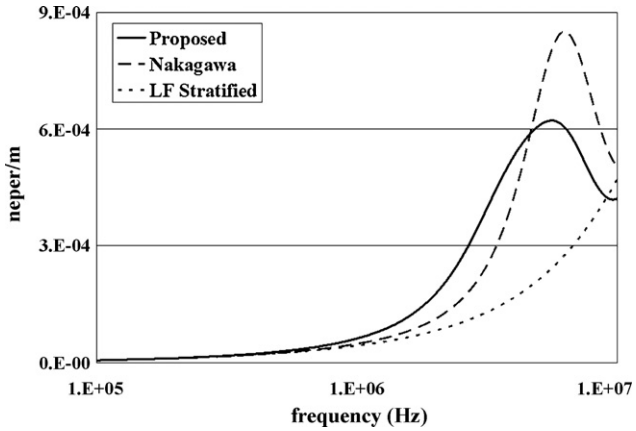

Fig. 10. Aerial mode #1 attenuation constant for different two-layer methods.

Although Nakagawa's model is an improvement to the LF model, the differences with the proposed model still remain significant, especially in the high frequency region. This is due to the increasing influence of the admittance earth correction terms, since the proposed and Nakagawa's models give identical results for the series impedances. The ground mode attenuation curve presents almost the same behavior as the corresponding of the LF Stratified model up to several MHz. However, in the upper frequency range a maximum peak point is recorded, due to the influence of earth permittivity on the series impedances.

The magnitude of the ground mode characteristic impedance is shown in Fig. 8. The three models show a significant different behavior, leading to considerable differences in the result. In Table 6, the corresponding relative differences are shown for different two-layer earth cases of Table 2, assuming $\rho_1 = 500\,\Omega$ m and $\rho_1 = 100\,\Omega$ m.

7. Remarks on the numerical results.

Summarizing the analysis for the homogeneous and the two-layer earth cases, the following remarks can be concluded.

- Modal attenuation constants of the proposed models are non-monotone functions of frequency, since they present a maximum peak value in the transition region.
- The proposed earth correction terms must be used for frequencies higher than $f_{cr,min}$ of the homogeneous earth or of one of the two layers.
- Carson's formula for the homogeneous earth can be only used in the low frequency region.
- Sunde's formulation for the homogeneous earth can be generally used only up to 1 MHz in cases of high earth resistivity and high earth permittivity.
- Depending on the characteristics of the earth layers of the two-layer earth, resonant oscillations may be observed.

Table 6
% Differences in the ground mode attenuation constant with different models. Two-layer earth case.

Cases	Frequencies			
	500 kHz	1 MHz	5 MHz	10 MHz
LF statified				
H1	24.61	40.73	10.62	224.98
H2	27.80	44.02	50.01	226.91
Nakagawa				
H1	27.18	51.37	48.71	62.64
H2	25.76	42.67	45.00	63.56

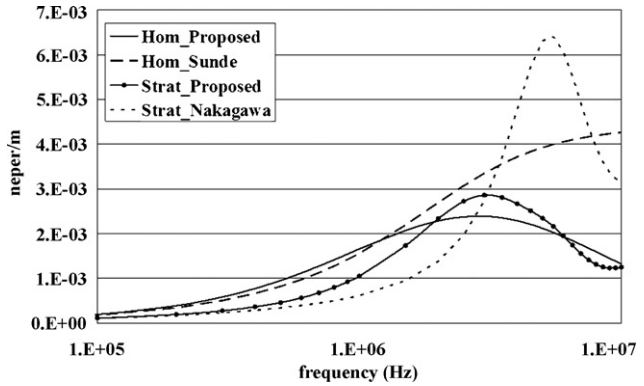

Fig. 11. Ground mode attenuation constants of the two-layer and homogeneous earth models.

8. Comparison of the two-layer with the homogeneous earth

The corresponding results for the stratified and the homogeneous earth topologies are compared in order to check the influence of earth stratification. For this purpose the proposed models for the two earth topologies, as well as the homogeneous earth and the two-layer earth models of Sunde and Nakagawa are chosen to be examined.

For the two-layer earth topology the depth of the first layer is $d = 5$ m, earth resistivities are $\rho_1 = 1000\,\Omega$ m and $\rho_2 = 100\,\Omega$ m and the relative permittivities of both layers are equal to 10, corresponding to case S1 of Table 2, while the homogeneous earth EM characteristics are assumed to be equal to those of the first layer, corresponding to case H1 of Table 2. The ground mode attenuation constant is presented in Fig. 11.

The differences in the results by the proposed method between the homogeneous and the stratified earth cases are shown in Fig. 12. They are calculated as percent using (8) with the homogeneous earth case as the reference. In the kHz frequency range differences are in average over 30% and tend to minimize, until the corresponding curves in Fig. 11 intersect. For higher frequencies, although differences have been reduced, they still remain significant and reach 20%. This is better explained if we consider the field penetration depth [4], given by (9). Fig. 13 shows the variation of the penetration depth with frequency and earth characteristics. The penetration depth tends asymptotically to non-zero values even in high frequencies, especially for cases of high earth resistivity. Therefore, although significant differences to the homogeneous earth case have been recorded for the earth return impedance [14]

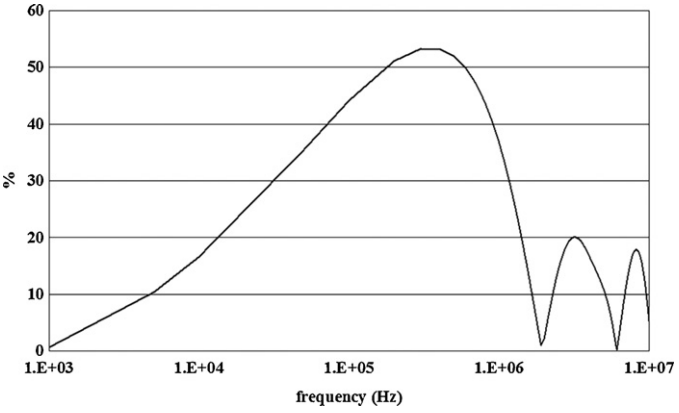

Fig. 12. Differences in the ground mode attenuation constant between the stratified and the homogeneous earth models.

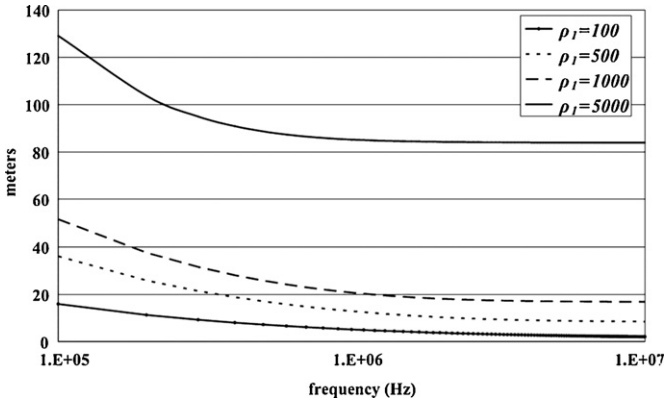

Fig. 13. Plot of the penetration depth vs. frequency for different earth resistivities. Relative earth permittivity is 10.

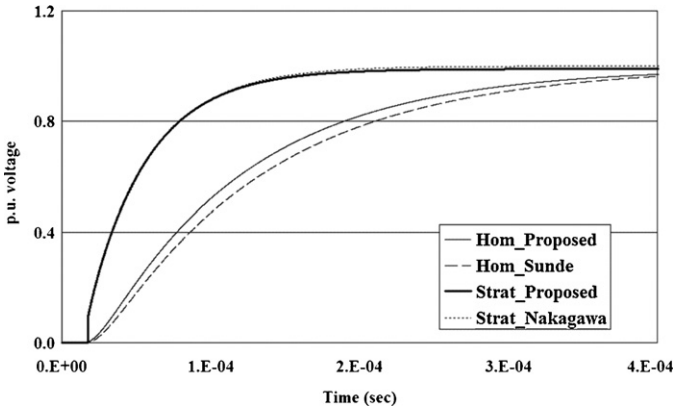

Fig. 14. Ground mode receiving end step voltage of different models.

and shunt admittance [16] in the kHz frequency range, the stratification of earth must be taken into account in the high frequency region as well.

$$\delta = \frac{1}{\omega\sqrt{\varepsilon_1\mu_1/2(\sqrt{1+(\sigma_1^2/(\omega^2\cdot\varepsilon_1^2))}-1)}}. \quad (9)$$

9. Transient responses

The propagation characteristics of the overhead transmission line of Fig. 4 are used in the simulation of fast transients in order to check the influence of the parameters, calculated by the proposed methodology on the transient response of the system.

The wave propagation characteristics of the overhead transmission line have been calculated for the same semi-infinite homogeneous and two-layer earth models as previous, assuming the same earth topologies and characteristics.

The time domain, distributed parameter traveling wave transmission line model of the ATP-EMTP [15] has been used. This model has been modified, using a cascaded series of line sections and adding shunt lumped resistances to simulate the conductance of the admittance earth correction terms. In order to check the validity of the modified model in high frequencies, results obtained for the steady state case using this model, were checked to those calculated by an exact frequency domain model using telegrapher's equations [19]. Negligible differences occurred, when the length of each cascaded equivalent line model is shorter than the wavelength of the applied voltage and the time step of the simulation procedure was is the order of nanoseconds.

9.1. Modal responses

First the equivalent single-phase circuit of the ground mode is considered, for a line length equal to 5 km, to allow very fast transients. A voltage step source with 1 pu magnitude is connected at the sending end *S* of the conductor, while the receiving end *R* is open ended. In Fig. 14 the recorded transient voltages at the line receiving end are presented.

Differences in the transient responses between the stratified and the homogeneous earth case are recorded, for both the proposed and the two approximate models. Comparing the proposed model results to the corresponding of Sunde and Nakagawa, significant differences are recorded especially for the homogeneous earth case, while for the stratified earth case the differences appear over a long time period.

9.2. Actual phase responses

Next, for the investigation of the actual transmission line transient response, the test configuration of Fig. 15 has been used.

The transmission line of Fig. 4 is considered with a length of 1 km. A double exponential voltage source with a magnitude of 1 pu and variable time constants is connected on the sending end *S* of conductor of phase *a*. Each conductor open terminal is terminated with its characteristic impedance [27].

The examined test cases and the recorded absolute differences in peak transient voltages indicating the quantitative influence of the different formulations are presented in Table 7. The percent differences are calculated keeping Sunde's model as the reference in all cases, since it is commonly used in surge type simulations [8]. In Figs. 16 and 17 the recorded transient voltages at the line receiving end *R*, for the different models are presented for the test cases A and D.

The comparison of the proposed model to Sunde's model for the homogeneous earth case leads to significant differences for cases B and D. These cases involve frequencies at the region where the modal propagation constants and especially the ground mode attenuation show a considerable divergence. The recorded differences vary for the different test cases. Sunde's model gives the worst transient in cases A and B, while in cases C and the proposed homogeneous model presents the worst transient voltages.

Comparing the two stratified earth models, significant differences on the transient voltages are also observed especially for the test case D. Furthermore, the two stratified earth models result in significantly different results to the homogeneous earth model, especially in cases of a very steep voltage ascent and therefore of transients in the higher frequency range. These results justify the need to include earth stratification in the transient transmission line model.

The most severe transients have been observed in cases A, B and C for Nakagawa's model, while in case D, the proposed two-layer earth model gives the worst transient. A direct interpretation of

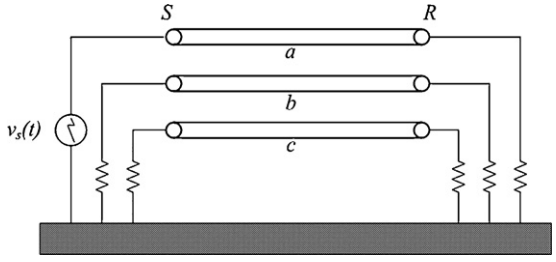

Fig. 15. Test configuration of the transient simulation.

Table 7
Peak relative (%) differences.

Test cases	Front time/tail time (μs)	% Differences		
		Proposed (homogeneous)	Nakagawa (stratified)	Proposed (stratified)
A	2/50	6.53	19.11	12.82
B	1/50	11.28	28.54	4.44
C	0.67/50	3.60	29.46	24.55
D	0.5/50	33.59	25.38	61.73

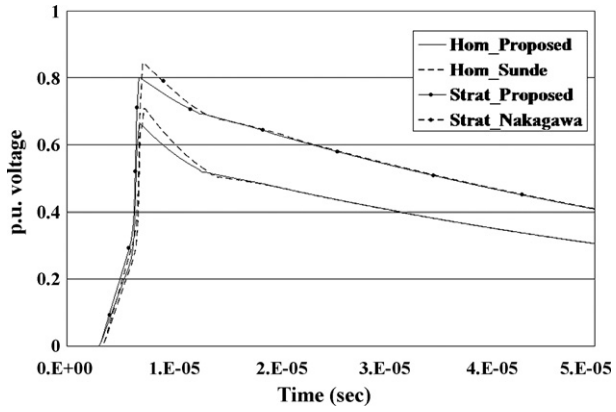

Fig. 16. Receiving end transient voltages of different models for case A.

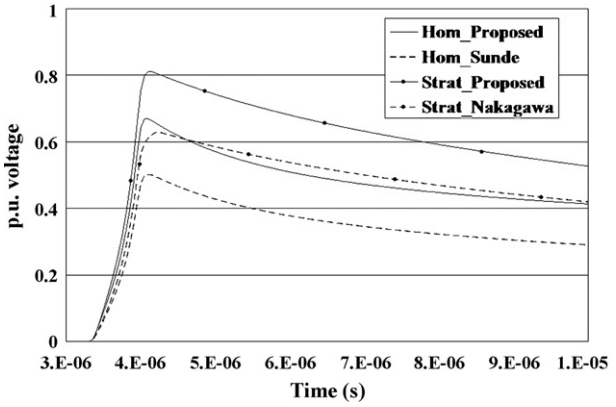

Fig. 17. Receiving end transient voltages of different models for case D.

the results is not easy, due to the complex differences in the modal propagation characteristics of the different models, especially in the high frequencies. However, the recorded differences in the transient responses justify the need for a more precise estimation of the transmission line model parameters.

10. Conclusion

A generalized formulation for the calculation of the influence of the imperfect earth on the series impedances and shunt admittances of overhead transmission lines in high frequencies for stratified earth cases is presented in this paper. Special emphasis is given to the influence of the axial displacement currents and the radial displacement and conducting currents. These currents must be taken into account in the high frequency region, the range of which depends on the electromagnetic characteristics of the earth.

The proposed generalized expressions, derived under the assumption of quasi-TEM propagation, can handle all practical cases of overhead multiconductor arrangements, taking into account the topology and the electromagnetic properties of all involved media. These expressions can include all existing approaches for the homogeneous and the two-layer earth cases, by the application of the corresponding assumptions. Finally, they may be also extended to include multi-layer horizontally stratified earth structures.

The propagation characteristics of a typical single-circuit three-phase overhead TL configuration has been analyzed for several earth topologies of arbitrary EM characteristics for a frequency range from 50 Hz to 10 MHz. The validity and accuracy of the proposed model has been verified, by comparing the obtained results with the corresponding by other known approaches.

From the comparative analysis of the results, it is shown that the influence of the earth permittivity for the line impedances and admittances must be taken into account. This is most evident in cases where the earth does not behave as a conductor but also as an insulator. Furthermore, earth stratification must be not omitted in the simulation of high frequency phenomena, especially when the penetration depth of the EM field extends deeper than the upper earth layer.

Finally, the influence of the parameters calculated by the proposed model on the transient response of a transmission line is checked, by simulating typical fast transient surges. Results show that the new correction terms introduced by the proposed models have a significant influence on the transient responses, especially in the MHz frequency range.

The proposed theoretical model together with the numerical integration scheme can be used for any type of overhead line configuration, offering a useful tool in the calculation of parameters of fast transient overhead line models and thus enhancing the simulation of various earth structures.

Acknowledgements

This work was supported by the Greek General Secretariat for Research and Technology (PENED 03). The helpful recommendations of Dr. D.A. Tsiamitros are greatly acknowledged by the authors.

Appendix A.

A.1. Determination of the dipole EM field

We assume a dipole with a moment *IdS* along the *x*-axis, placed in the height $h = h_i$ of conductor *i* over a two-layer earth, as shown in Fig. 18. Since the field is symmetrical with respect to the *x*–*z* plane, the *y* component Π'_y is zero. The *x*- and *z*-components of the resultant Herzian vector in the air, the first layer and the second layer are Π'_{0x}, Π'_{0z}, Π'_{1x}, Π'_{1z} and Π'_{2x}, Π'_{2z}, respectively. Their analytical expressions are:

A.1.1. Air ($z \geq d$)

$$\Pi'_{0x} = \int_0^\infty \left[C \frac{u}{a'_0} e^{-a'_0|z-(d+h)|} + g_0 \cdot e^{-a'_0 z} \right] J_0(ru)du, \tag{A.1a}$$

$$\Pi'_{0z} = \frac{x}{r} \int_0^\infty p_0 \cdot e^{-a'_0 z} \cdot J_1(ru)du. \tag{A.1b}$$

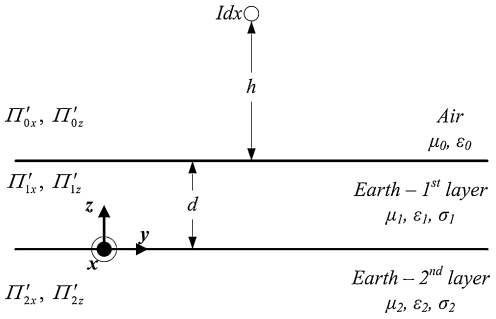

Fig. 18. Dipole configuration over a two-layer earth.

A.1.2. First earth layer ($0 \le z < d$)

$$\Pi'_{1x} = \int_0^\infty \left[f_1 \cdot e^{a'_1 z} + g_1 \cdot e^{-a'_1 z} \right] J_0(ru)du, \tag{A.2a}$$

$$\Pi'_{1z} = \frac{x}{r} \int_0^\infty \left[p_1 \cdot e^{a'_1 z} + q_1 \cdot e^{-a'_1 z} \right] J_1(ru)du. \tag{A.2b}$$

A.1.3. Second earth layer ($z < 0$)

$$\Pi'_{2x} = \int_0^\infty f_2 \cdot e^{a'_2 z} \cdot J_0(ru)du, \tag{A.3a}$$

$$\Pi'_{2z} = \frac{x}{r} \int_0^\infty p_2 \cdot e^{a'_2 z} \cdot J_1(ru)du. \tag{A.3b}$$

In the above equations, the prime indicates the Herzian vector of the dipole, as opposed to that of an infinite line. $J_0(\,)$ and $J_1(\,)$ are the Bessel functions of the first kind and zero and first order, respectively, $\gamma_k^2 = j\omega\mu_k(\sigma_k + j\omega\varepsilon_k)$, $a'_k = \sqrt{u^2 + \gamma_k^2}$, where $k = 0, 1, 2$, $r = \sqrt{x^2 + y^2}$, $\cos\varphi = x/r$, j is the imaginary unit, u the integral variable and C is equal to $I \cdot dS \cdot j\omega\mu_0/4\pi\gamma_0^2$.

The unknown functions f and g in Eqs. (A.1)–(A.3) are obtained from the boundary conditions between the different media. The boundary conditions between two horizontal media a and b are generally defined as [14]:

$$\gamma_a^2 \cdot \Pi'_{ax} = \gamma_b^2 \cdot \Pi'_{bx}, \tag{A.4a}$$

$$\frac{\gamma_a^2}{\mu_a} \cdot \frac{\partial \Pi'_{ax}}{\partial z} = \frac{\gamma_b^2}{\mu_b} \cdot \frac{\partial \Pi'_{bx}}{\partial z}, \tag{A.4b}$$

$$\frac{\gamma_a^2}{\mu_a} \Pi'_{az} = \frac{\gamma_b^2}{\mu_b} \Pi'_{bz}, \tag{A.4c}$$

$$\frac{\partial \Pi'_{ax}}{\partial x} + \frac{\partial \Pi'_{az}}{\partial z} = \frac{\partial \Pi'_{bx}}{\partial x} + \frac{\partial \Pi'_{bz}}{\partial z}. \tag{A.4d}$$

The above set of equations is applied to each separating surface at $z = d$ and $z = 0$. First, the x-components are determined separately and then are used in finding the z-components. Therefore, substituting (A.1a), (A.2a), and (A.3a) in (A.4a) and (A.4b) and also (A.1b), (A.2b), and (A.3b) in (A.4c) and (A.4d) the unknown functions g_0 and p_0 of (A.1a) and (A.1b), respectively are derived in (A.5a) and (A.5b).

$$g_0 = \frac{Cu}{a_0} \cdot e^{-a'_0(h-d)} \cdot T'_1, \tag{A.5a}$$

$$p_0 = 2Cu^2 \cdot e^{-a'_0(h-d)} \cdot T'_2, \tag{A.5b}$$

T'_1 and T'_2 are given in (A.6a) and (A.6b), respectively, while their components are presented in (A.7).

$$T'_1 = \frac{\Delta'_1}{\Delta'} = \frac{d'_{01}s'_{12} + s'_{01}d'_{12}e^{-2a'_1 d}}{s'_{01}s'_{12} + d'_{01}d'_{12}e^{-2a'_1 d}}, \tag{A.6a}$$

$$T'_2 = \frac{\mu_0\mu_1(\gamma_0^2 - \gamma_1^2)[s'_{12} + d'_{12}e^{-2a'_1 d}][S'_{12} + D'_{12}e^{-2a_1 d}] - 4\mu_0\mu_1^2\mu_2 a'^2_1\gamma_0^2 e^{-2a_1 d}(\gamma_2^2 - \gamma_1^2)}{\Delta'_2 \cdot \Delta'}, \tag{A.6b}$$

$$\Delta' = s'_{01}s'_{12} + d'_{01}d'_{12}e^{-2a'_1 d}, \tag{A.7a}$$

$$\Delta_1 = d'_{01}s'_{12} + s'_{01}d'_{12}e^{-2a'_1 d}, \tag{A.7b}$$

$$\Delta'_2 = S'_{01}S'_{12} + D'_{01}D'_{12}e^{-2a_1 d}. \tag{A.7c}$$

$$s'_{mn} = (a'_m\mu_n + a'_n\mu_m), \tag{A.7d}$$

$$d'_{mn} = (a'_m\mu_n - a'_n\mu_m), \tag{A.7e}$$

$$S'_{mn} = (\mu_m\gamma_n^2 a'_m + \mu_n\gamma_m^2 a'_n), \tag{A.7f}$$

$$D'_{mn} = (\mu_m\gamma_n^2 a'_m - \mu_n\gamma_m^2 a'_n), \tag{A.7g}$$

where the m, n indices, take the values 0, 1, 2, corresponding to the air and the two earth layers, respectively.

Thus, the Π' function in the air is completely defined and (A.1a) and (A.1b) take the following respective form:

$$\Pi'_{0x} = \int_0^\infty \left(\frac{Cu}{a'_0} e^{-a'_0|z-(d+h)|} + \frac{Cu}{a'_0} e^{-a'_0(h+z-d)} \cdot T'_1 \right) J_0(ru)du, \tag{A.8a}$$

$$\Pi'_{0z} = \frac{x}{r} \int_0^\infty 2Cu^2 \cdot T'_2 \cdot e^{-a'_0(h+z-d)} J_1(ru)du. \tag{A.8b}$$

Next, the x and y components of the electric field intensity are expressed in rectangular coordinates and are defined by the wave function Π and the intermediate functions $P(r)$ and $Q(r)$ in (A.9a) and (A.9b) [5].

$$E_x = -\gamma_0^2\Pi'_{0x} + \frac{\partial}{\partial x}\left[\frac{\partial \Pi'_{0x}}{\partial x} + \frac{\partial \Pi'_{0z}}{\partial z} \right] = IdS\left[-P(r) + \frac{\partial^2 Q(r)}{\partial x^2} \right], \tag{A.9a}$$

$$E_y = \frac{\partial}{\partial y}\left[\frac{\partial \Pi'_{0x}}{\partial x} + \frac{\partial \Pi'_{0z}}{\partial z} \right] = IdS\frac{\partial^2 Q(r)}{\partial x \partial y}, \tag{A.9b}$$

$P(r)$ and $Q(r)$ are used in the determination of the pul earth correction terms of a line with an infinite length in the following expressions [5]:

$$Z'_{e_{ij}}(\gamma_x) = \int_{-\infty}^{\infty} P(\sqrt{x^2 + y^2}) e^{-\gamma_x x} dx, \tag{A.10a}$$

$$Y'^{-1}_{e_{ij}}(\gamma_x) = \int_{-\infty}^{\infty} Q(\sqrt{x^2 + y^2}) e^{-\gamma_x x} dx, \tag{A.10b}$$

Substituting in (A.9) Eqs. (A.8a) and (A.8b) and using (A.11), (4a) and (4b) are derived.

$$\frac{\partial J_0(ru)}{\partial x} = -\cos\varphi \cdot u \cdot J_1(ru), \tag{A.11}$$

A.2. Derivation of the impedance and admittance formulas

Since γ_x is equal to jk_0, the second integral of (4) can be calculated using (A.9) [14].

$$\int_{-\infty}^{\infty} J_0\left(u\sqrt{x^2 + y_{ij}^2}\right) e^{-jk_0 x} dx = \begin{cases} 0, & u < k_0 \\ 2\dfrac{\cos\left(y_{ij}\sqrt{u^2 - k_0^2}\right)}{\sqrt{u^2 - k_0^2}}, & u > k_0 \end{cases}, \tag{A.12}$$

Assuming the relation $u^2 - k_0^2 = \lambda^2$, the terms a'_k for $k = 0, 1, 2$ transform to $a_k = \sqrt{\lambda^2 + \gamma_k^2 + k_0^2}$, T'_1 and T'_2 to T_1 and T_2, respectively. Using (A.9) and the above transformations the pu length mutual

impedances and admittances for the two-layer earth structure take the form of (5) and (6), respectively. The logarithmic terms of (5) and (6) are derived, using (A.10) [14].

$$\int_0^\infty \left(\frac{e^{-\alpha'_0 \left| h_j - h_i \right|}}{a'_0} + \frac{e^{-\alpha'_0 (h_i + h_j)}}{a'_0} \right) \cos(y_{ij}\lambda) d\lambda = \ln \frac{D_{ij}}{d_{ij}}, \qquad \text{(A.13)}$$

where $D_{ij} = \sqrt{y_{ij}^2 + (h_i + h_j)^2}$, $d_{ij} = \sqrt{y_{ij}^2 + (h_i - h_j)^2}$.

References

[1] J.R. Carson, Wave propagation in overhead wires with ground return, Bell Syst. Tech. J. (5) (1926) 539–554.
[2] M.C. Perz, M.R. Raghuveer, Generalized derivation of fields, and impedance correction factors of lossy transmission lines. Part II. Lossy conductors above lossy ground, IEEE Trans. Power Syst. 93 (6) (1974) 1832–1841.
[3] L. Hofman, Series expansions for line series impedances considering different specific resistances, magnetic permeabilities, and dielectric permittivities of conductors, air, and ground, IEEE Trans. Power Deliv. 18 (2) (2003) 564–570.
[4] A. Semlyen, Ground return parameters of transmission lines an asymptotic analysis for very high frequencies, IEEE Trans. Power Syst. 100 (3) (1981) 1031–1038.
[5] E.D. Sunde, Earth Conduction Effects in Transmission Systems, 2nd ed., Dover Publications, 1968, pp. 99–139.
[6] F. Rachidi, C.A. Nucci, M. Ianoz, Transient analysis of multiconductor lines above a lossy ground, IEEE Trans. Power Deliv. 14 (1) (1999) 294–302.
[7] N. Theethayi, R. Thottappillil, Y. Liu, R. Montano, Important parameters that influence crosstalk in multiconductor transmission lines, Electr. Power Syst. Res. (2006), doi:10.1019/j.epsr.2006.06.014.
[8] F. Rachidi, C.A. Nucci, M. Ianoz, C. Mazzeti, Influence of a lossy ground on lightning-induced voltages on overhead lines, IEEE Trans. EMC 38 (3) (1996) 250–264.
[9] W.H. Wise, Propagation of high frequency currents in ground return circuits, Proc. Inst. Radio Eng. (22) (1934) 522–527.
[10] W.H. Wise, Effect of ground permeability on ground return circuits, Bell Syst. Tech. J. (10) (1931) 472–484.
[11] W.H. Wise, Potential coefficients for ground return circuits, Bell Syst. Tech. J. 27 (1948) 365–371.
[12] M. Nakagawa, Admittance correction effects of a single overhead line, IEEE Trans. Power Syst. PAS-100 (3) (1981) 1154–1161.
[13] M. Nakagawa, Further Studies on wave propagation along overhead transmission lines: effects of admittance correction, IEEE Trans. Power Syst. PAS-100 (7) (1981) 3626–3633.
[14] N. Nakagawa, A. Ametani, K. Iwamoto, Further studies on wave propagation in overhead lines with earth return: impedance of stratified earth, Proc. IEE 120 (12) (1973) 1521–1528.
[15] H.W. Dommel, Electromagnetic Transients Program Reference Manual, Bonneville Power Administration, Portland, OR, 1986.
[16] A. Ametani, N. Nagaoka, R. Koide, Wave propagation characteristics on an overhead conductor above snow, Trans. Inst. Electr. Eng. Jpn. 134 (3) (2001) 26–33.
[17] H. Kikuchi, Wave propagation along an infinite wire above ground at high frequencies, Electrotech. J. Jpn. 2 (1956) 73–78.
[18] A.E. Efthymiadis, L.M. Wedepohl, Propagation characteristics of infinitely – long single – conductor lines by the complete field solution method, Proc. IEE 125 (6) (1978) 511–517.
[19] F.M. Tesche, M. Ianoz, T. Karlsson, EMC Analysis methods and Computational Models, John Wiley and Sons Inc., 1997, pp. 405–411.
[20] P. Pettersson, Image representation of wave propagation on wires above, on and under ground, IEEE Trans. Power Deliv. 9 (2) (1994) 1049–1055.
[21] M. D'Amore, M.S. Sarto, Simulation models of a dissipative transmission line above a lossy ground for a wide-frequency range. Part I: Single conductor configuration, IEEE Trans. EMC 38 (2) (1996) 127–138.
[22] M. D'Amore, M.S. Sarto, Simulation models of a dissipative transmission line above a lossy ground for a wide-frequency range. Part II: Multiconductor configuration, IEEE Trans. EMC 38 (2) (1996) 139–149.
[23] J.R. Wait, Theory of wave propagation along a thin wire parallel to an interface, Radio Sci. 7 (6) (1972) 675–679.
[24] P. Degauque, G. Courbet, M. Heddebaut, Propagation along a line parallel to the ground surface: comparison between the exact solution and the quasi-TEM approximation, IEEE Trans. EMC vol.25 (4) (1983) 422–427.
[25] G.E.J. Bridges, L. Shafai, Plane wave coupling to multiple conductor tranmission lines above a lossy earth, IEEE Trans. EMC vol.31 (1) (1989) 21–33.
[26] G.K. Papagiannis, D.A. Tsiamitros, D.P. Labridis, P.S. Dokopoulos, A systematic approach to the evaluation of the influence of multilayered earth on overhead power transmission lines, IEEE Trans. Power Deliv. 20 (4) (2005) 2594–2601.
[27] L.M. Wedepohl, Application of the solution of travelling wave phenomena in polyphase system, Proc. IEE 110 (December (12)) (1963) 2200–2212.
[28] A. Ametani, A general formulation of impedance and admittance of cables, IEEE Trans. Power Appar. Syst. PAS-99 (3) (1980) 902–910.
[29] R.G. Olsen, J.L. Young, D.C. Chang, Electromagnetic wave propagation on a thin wire above earth, IEEE Trans. Antennas Propag. 48 (9) (2000) 1413–1419.
[30] T.A. Papadopoulos, G.K. Papagiannis, "Influence of Earth Permittivity on Overhead Transmission Line Earth-Return Impedances," presented at 2007 IEEE Lausanne PowerTech Conf., Lausanne, Switcherland, 2007.
[31] P. Amirshahi, M. Kavehrad, High-Frequency characteristics of overhead multiconductor power lines for broadband communications, IEEE J. Selected Areas Commun. 24 (7) (2006).
[32] A. Ametani, Stratified earth effects on wave propagation—frequency-dependent parameters, IEEE PAS PAS-93 (5) (1974) 1233–1239.

Theofilos A. Papadopoulos was born in Thessaloniki, Greece, on March 10, 1980. He received his Dipl. Eng. Degree from the Department of Electrical and Computer Engineering at the Aristotle University of Thessaloniki, in 2003. Since 2003 he is a postgraduate student at the Department of Electrical and Computer Engineering at the Aristotle University of Thessaloniki. His special interests are power systems modeling, power-line communications and computation of electromagnetic transients. Mr. Papadopoulos has received the Basil Papadias Award for the best student paper, presented at the IEEE PowerTech '07 Conference in Lausanne, Switzerland.

Grigoris K. Papagiannis was born in Thessaloniki, Greece, on September 23, 1956. He received his Dipl. Eng. Degree and his Ph.D. degree from the Department of Electrical and Computer Engineering at the Aristotle University of Thessaloniki, in 1979 and 1998, respectively.

He is currently As. Professor at the Power Systems Laboratory of the Department of Electrical and Computer Engineering of the Aristotle University of Thessaloniki, Greece. His special interests are power systems modeling, computation of electromagnetic transients, distributed generation and power-line communications.

Dimitris P. Labridis was born in Thessaloniki, Greece, on July 26, 1958. He received the Dipl.-Eng. degree and the Ph.D. degree from the Department of Electrical and Computer Engineering at the Aristotle University of Thessaloniki, in 1981 and 1989, respectively. Currently he is a Professor at the same Department. His special interests are power system analysis with special emphasis on the simulation of transmission and distribution systems, electromagnetic and thermal field analysis, artificial intelligence applications in power systems, power-line communications and distributed energy resources.